Vol. 91 No. 2 pp. 711–726 ACTA GEOLOGICA SINICA (English Edition) Apr. 2017

Germanium in Magnetite: A Preliminary Review

MENG Yumiao, HU Ruizhong, HUANG Xiaowen* and GAO Jianfeng

State Key Laboratory of Ore Deposit Geochemistry, Institute of Geochemistry, Chinese Academy of Sciences, Guiyang 550081, China

Abstract: Magnetite is a very common mineral in various types of iron deposits and some sulfide deposits. Recent studies have focused on the use of trace elements in magnetite to discriminate ore types or trace ore-forming process. Germanium is a disperse element in the crust, but sometimes is not rare in magnetite. Germanium in magnetite can be determined by laser ablation ICP-MS due to its low detection limit (0.0X ppm). In this study, we summary the Ge data of magnetite from magmatic deposits, iron formations, skarn deposits, iron oxide copper-gold deposits, and igneous derived hydrothermal deposits. Magnetite from iron formations contains relatively high Ge (up to ~250 ppm), whereas those from all other deposits mostly contains Ge less than 10 ppm, indicating that iron formations can be discriminated from other Fe deposits by Ge contents. Germanium in magmatic/ hydrothermal magnetite is controlled by a few factors. Primary magma/fluid composition may be the major control of Ge in magnetite. Higher oxygen fugacity may be beneficial to Ge partition into magnetite. Sulfur fugacity and temperature may have little effect on Ge in magnetite. The enrichment mechanism of Ge in magnetite from iron formations remains unknown due to the complex ore genesis. Germanium along with other elements (Mn, Ni, Ga) and element ratios (Ge/Ga and Ge/Si raios) can distinguish different types of deposits, indicating that Ge can be used as a discriminate factor like Ti and V. Because of the availability of in situ analytical technique like laser ablation ICP-MS, in situ Ge/ Si ratio of magnetite can serve as a geochemical tracer and may provide new constraints on the genesis of banded iron formations.

Key words: germanium, magnetite, controlling factor, iron deposits, discriminate factor

1 Introduction

Magnetite (Fe_3O_4) is a common mineral in a variety of rocks and deposits. Trace elements of magnetite have been widely used to study petrogenesis and ore genesis (e.g., Dupuis and Beaudoin, 2011; Huang et al., 2013b, 2015a, 2015b, 2016; Dare et al., 2014; Nadoll et al., 2014, 2015). The improvement of analytical techniques such as laser ablation inductively coupled plasma mass spectrometry (LA-ICP-MS) and trace mode electron microprobe allow in situ measurements of trace elements with increasingly lower detection limits (e.g., Longerich et al., 1996; Norman et al., 1996; Liu et al., 2008; Dupuis and Beaudoin, 2011; Nadoll and Koenig, 2011). Previous studies have focused on elements such as Al, Ti, Mg, Mn, Zn, Cr, V, Ni, Co, and Ga that are called spinel elements. The content variation of these elements commonly indicates the various formation conditions, which has been used in provenance studies of iron oxide and sulfide deposits. Germanium shows distinctly lithophile, siderophile, chalcophile, and organophile behaviors in different environments (Bernstein, 1985). Germanium in magnetite thus can be used to discuss the formation conditions of magnetite and the deposits. In this paper, we review Ge in magnetite from a variety of ore deposits, including (1) magmatic iron oxide and sulfide deposits, (2) iron formations, (3) skarn Fe deposits, (4) iron oxide copper-gold deposits, and (5) igneous derived hydrothermal deposits. The possible factors controlling Ge in magnetite and application of Ge to discriminate different deposit types are also discussed.

1.1 Fundamental properties and distribution of Ge

Germanium is a typical dispersed element in the earth, with similar concentration of ~1.1–1.6 ppm in primitive mantle, ocean crust and continental crust (Taylor and McLennan, 1985; Dasch, 1996). In the earth's crust, most

* Corresponding author. E-mail: huangxiaowen@vip.gyig.ac.cn

Ge is dispersed through silicate minerals in amounts up to a few parts per million due to isomorphous substitution of Ge^{4+} for the chemically similar Si^{4+} (Bernstein, 1985). Ge is mainly associated with minerals or ores containing Si, C, Zn, Cu, Fe, Sn, and Ag (Rosenberg, 2009). Ge occurs in the oxidation states +2 and +4, where the latter possesses the higher stability. In minerals, Ge often appears in the form of the oxide (GeO_2) or the sulfide (GeS_2), and in solution as germanic acid, $Ge(OH)_4$ (Rosenberg, 2009). Germanium exhibits siderophile, lithophile, chalcophile and organophile behaviors in different geologic environments (Höll et al., 2007).

The special geochemical properties control the distribution of Ge in geological environments. Germanium is found to be hosted in different types of rocks. Ultramafic rocks, mafic rocks, granites, shales, and deep-sea clays have similar Ge contents ranging from 1.3 to 2 ppm (Faure, 1998; Reimann and Caritat, 1998). Sandstones and carbonates are relatively depleted in Ge with average contents of 0.8 ppm and 0.2 ppm, respectively (Faure, 1998). Germanium is also hosted in (1) zinc or copper-rich sulfide deposits and their oxidized products, particularly for those hosted in sedimentary rocks, (2) lignite and coal deposits, (3) iron oxide deposits (Hu Ruizhong et al., 2000; Höll et al., 2007). The concentration of Ge in these deposits ranges from <1 ppm to several percent. Germanium occurs as independent Ge minerals or trace element in other minerals. The common Ge minerals such as argyrodite, briartite, germanite, renierite, and stottite contain 4wt%–32wt% Ge (Höll et al., 2007). Low-iron sphalerite is the most important Ge-rich mineral with Ge concentration of up to 3000 ppm (Höll et al., 2007). Besides sphalerite, sulfides such as enargite, stannite, canfieldite, and colusite are also important Ge-bearing minerals, all of which have sphalerite or wurtzite-derivative structures with quadrivalent Ge in tetrahedral sites (Höll et al., 2007). These minerals contain 100–2800 ppm Ge (Höll et al., 2007; Belissont et al., 2014; Cook et al., 2015). Germanium is also hosted in oxide and hydroxide minerals. For example, cassiterite from porphyry and vein–stockwork Sn–Ag deposits contains up to 3000 ppm Ge (Bernstein, 1985). Goethite from oxide zone of Apex mine contains up to 5000 ppm Ge (Bernstein, 1985). Iron oxides such as magnetite and hematite are very common in Fe deposits, but the Ge contents of these minerals are rarely reported.

There are a few data regarding Ge in Fe-oxide ores and Fe oxides before the 2000s. Germanium was mainly enriched in oxide facies rather than silicate, carbonate, and sulfide facies of Banded Iron Formations (BIF) (Saprykin, 1977). Oxide ores contain up to 38 ppm Ge in BIF from the Hamersley Range, Australia (Davy, 1983). Those from Kremenchuk-Krivoi Rog, Ukraine have similar Ge contents, with average contents of 27 ppm and 43 ppm in hematite and magnetite, respectively (Saprykin, 1977). In contrast, oolitic Fe-ores (e.g., Minette ores in France, and Salzgitter ores in Germany) are poor in Ge (<10 ppm) (Hörmann, 1963; De Argollo and Schilling, 1978). Hematite and magnetite from the small Lahn–Dill-type deposits in Germany contain up to 20 ppm Ge (average 8 ppm Ge) and up to 100 ppm Ge (average 40 ppm Ge), respectively (Schrön, 1968; De Argollo and Schilling, 1978). Magnetite from the magnetite–hematite ores of (metamorphosed) volcanogenic–sedimentary deposits has an average Ge concentration of 10 ppm, whereas those from the skarn deposits contain ~2.5 ppm Ge (Vakrushev and Semenov, 1969). Bekmukhametov et al. (1973) founded that there are up to 70 ppm Ge in magnetite–hematite of volcanogenic–sedimentary origin, up to 20 ppm Ge in magnetite from vein deposits, up to a few ppm in Fe-oxides from skarns, and up to several ppm from supergene limonites within Fe deposits from Kazakhstan.

1.2 Mineralogy and crystallography of magnetite

Nadoll et al. (2014) have reviewed the chemistry of hydrothermal magnetite, as well as the mineralogy and crystallography of magnetite. Here, we emphasis Ge in mineral structure of magnetite. Magnetite has an inverse spinel structure with the general stoichiometry AB_2O_4 (Fleet, 1981), where A represents a divalent cation such as Mg, Fe^{2+}, Ni, Mn, Co, or Zn, and B represents a trivalent cation such as Al, Fe^{3+}, Cr, V, Mn, or Ga (Lindsley, 1976; Wechsler et al., 1984). Ti^{4+} can also occupy the B site when substitution is coupled with a divalent cation (Wechsler et al., 1984). Octahedral sites in the magnetite structure are randomly occupied by subequal numbers of ferric (Fe^{3+}) and ferrous (Fe^{2+}) iron atoms, whereas tetrahedral sites are exclusively occupied by the smaller ferric iron atoms $Fe^{3+}[Fe^{2+}Fe^{3+}]O_4$ (Lindsley, 1976; Wechsler et al., 1984).

Germanium has the outer-electron configuration $3d^{10}4s^24p^2$ and generally occurs in the quadrivalent state (Bernstein, 1985). The relatively high electronegativity of Ge leads to the formation of predominately covalent bonds with many ligands. For example, Ge-O bonds have roughly 31% ionic character and Ge-S bonds have only 7% (Bernstein, 1985). According to Goldschmidt's rule, the incorporation of foreign cations is more likely when the substituting cation has a similar charge and ionic radius (±15%–18% radius variations). Ge^{4+} in tetravalent coordination has the ion radius of 0.39 nm, out of the ±15%–18% radius variations of 0.49 nm for Fe^{3+} in the same coordination (Shannon, 1976). Ge^{4+} in hexavalent coordination has the ion radius of 0.53 nm, also out of the

±15%–18% radius variations of 0.65 nm and 0.78 nm for Fe^{3+} and Fe^{2+}, respectively, in the same coordination (Shannon, 1976). Therefore, single atom substitution of Fe^{2+} or Fe^{3+} by Ge^{4+} is hardly possible. Alternatively, coupled substitution of Fe^{3+} by Ge^{4+} and other ions is more likely, i.e. $Ge^{4+} + Fe^{2+} \rightarrow 2Fe^{3+}$.

Solid solution between magnetite and brunogeierite may also exist and can be represented by $(Ge^{4+}_{1-x}Fe^{3+}_{x})(Fe^{2+}_{2-x}Fe^{3+}_{x})O_4$ (Ottemann and Nuber, 1972). Brunogeierite (Fe_2GeO_4) in the sphalerite deposits at Pyrenees and Tsumeb has a spinel structure. The synthetic equivalent of brunogeierite was proved to have a normal spinel with Ge^{4+} in tetravalent coordination and Fe^{2+} in octahedral coordination (Durif-Varambon et al., 1956; Rossiter, 1966). Therefore, the Ge-rich magnetite in some special environments probably reflects the solid solution between magnetite and brunogeierite. This needs the further work.

2 Methodology

LA-ICP-MS is a rapid and precise method for in situ determination of trace element abundances in magnetite. This technique has the advantages of a spatial resolution of < 0.1 mm, sub-ppm detection limits for a variety of elements, and rapid analysis times (typically < 2 minutes per point analysis).

Data summarized in this review are acquired by two methods. The first method was detailedly described in Dare et al. (2012) and is simply introduced here. ^{57}Fe was used as the internal standard and the stoichiometric value of Fe is assumed to be 72.4wt%. All data was reduced using Plasma Lab software (Thermo Elemental). A series of Fe-bearing international reference materials, BCR2-g, NIST361 and MASS-1, was used for the calibration of the LA-ICP-MS. A komatiitic glass (GOR-128g) and a natural magnetite (BC28) from the Bushveld Complex were used to monitor the data quality by analyzing them as unknown samples each run. The results of the monitors are generally within 10% analytical error of the working values and relative standard deviation (RSD) is typically less than 10%. The detection limit of Ge is 0.093 ppm.

The second method was detailedly described in Gao et al. (2013) and Huang et al. (2013b) and widely used in recent papers (Huang Xiaowen et al., 2014a; Huang et al., 2015a, b; Chen et al., 2015a, c; Chung et al., 2015; Liu et al., 2015; Zhao and Zhou, 2015). Offline data was reduced by ICPMSDataCal (Liu et al., 2008), including integration selection of background and analysis signals, time drift correction, and quantitative calibration. Element contents were calibrated against multiple reference materials (GSE-1G, BCR-2G, BIR-1G, and BHVO-2G) using ^{57}Fe as the internal standard. The sum of all element concentrations expressed as oxides (according to their oxidation states in magnetite) are considered to be 100wt% for a given anhydrous mineral (Liu et al., 2008). The detection limit of Ge is commonly lower than 0.4 ppm.

3 Ge Geochemistry of Magnetite

3.1 Ge content in magnetite from various deposits

3.1.1. Magmatic Fe and sulfide deposits

(1) Fe-Ti-(V) deposits

The Taihe, Baima, Hongge, Panzhihua and Anyi intrusions of the Emeishan Large Igneous Province (ELIP), SW China, contain large magmatic Fe–Ti–(V) oxide deposits. Because magnetite has extensive trellis or sandwich exsolution lamellae of ilmenite and spinel, LA-ICP-MS can provide more homogenous composition than EMPA that represents the primary composition of magnetite. Magnetites from these intrusions contain similar Ge contents ranging from 0.05 to 1.11 ppm (Fig. 1a), slightly lower than or nearly equal to the average Ge content (1.3 ppm) of bulk continental crust (Rudnick and Gao, 2003). Similar multi-element variation patterns of magnetite and bi-modal distribution of the highly compatible V and Cr in magnetite from Fe–Ti oxide ores of the ELIP indicate that magnetite may not form from fractional crystallization, but from relatively homogeneous Fe-rich melts (Liu et al., 2015). QUILF equilibrium modeling further indicates that magnetite of the Panzhihua and Baima intrusions crystallized under high oxygen fugacities, whereas those of Taihe, Hongge and Anyi intrusions crystallized under relatively low oxygen fugacities (Liu et al., 2015). In general, magnetite from Panzhihua and Baima intrusions has slightly higher average Ge contents than those from other three intrusions of the ELIP, indicating that higher oxygen fugacities may be beneficial to Ge partition into magnetite.

(2) Fe-Ti-P deposits

Dare et al. (2014) summarized the trace element composition of magnetite from Fe-Ti-P deposit or mineralization hosted in the Bushveld Complex of South Africa, the Sept-Iles Intrusive Suite of Canada, and the St. Charles de Bourget of Canada. Magnetite from these layered intrusions or massive nelsonite dykes has exsolutions of ilmenite and Mg-Al rich spinel. Magnetite of Fe-Ti-P ores from these rocks contains 0.69–1.40 ppm Ge with an average value of 0.99 ppm (Fig. 1a) (Dare et al., 2014), similar to those of magmatic Fe-Ti-(V) deposits.

The ~1.74 Ga Damiao anorthosite complex in northern part of the North China Craton hosts more than 130 Fe-Ti-P ore bodies, as pods, lenses, veins and dykes or stockworks, up to tens of meters wide (Chen et al., 2015b). These orebodies are mainly hosted in anorthosite

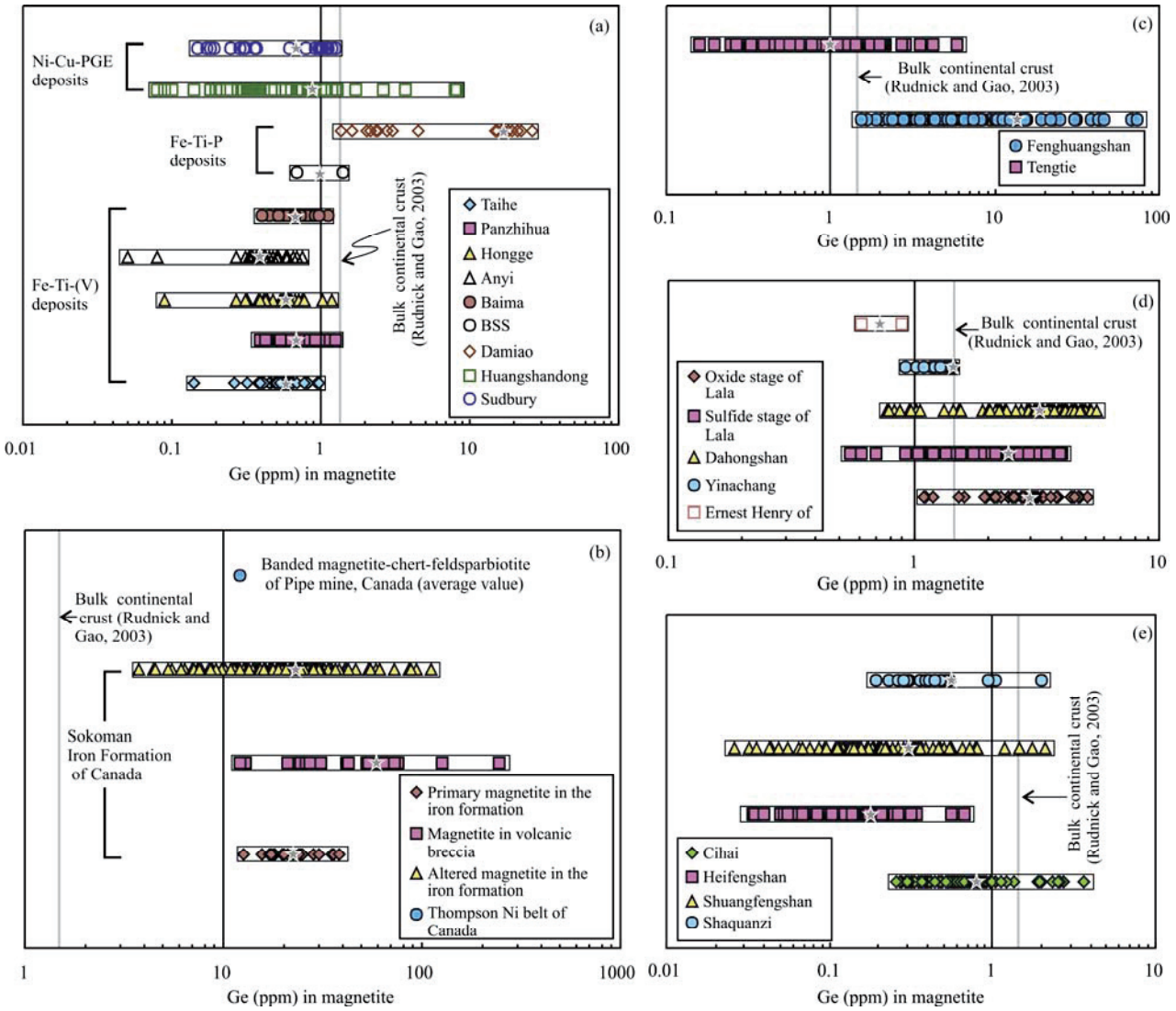

Fig. 1. Ge contents of magnetite from (a) magmatic Fe-Ti-(V), Fe-Ti-P and Ni-Cu-PGE deposits, (b) iron formations, (c) skarn Fe deposits, (d) iron oxide copper-gold deposits, (e) igneous derived hydrothermal Fe deposits.

Legend "BSS" in *a* represent three locations, Bushveld Complex of south Africa, Sept Iles of Canada, and Chales de Bourget of Canada. Two Ge data of magnetite from Ernest Henry deposit of Canada in *d* represent the minimum and maximum values of Ge contents. Pentagen filled by gray represents the average Ge content for individual deposit, similarly hereinafter. Data sources: magmatic deposits (Dare et al., 2012, 2014; Liu et al., 2015), iron formations (Dare et al., 2014; Chung et al., 2015), skarn Fe deposits (Zhao and Zhou, 2015; Huang et al., 2016), iron oxide copper-gold deposits (Dare et al., 2014; Chen et al., 2015a), igneous derived hydrothermal Fe deposits (Huang et al., 2013b, 2014a). The Ge content of bulk continental crust is referenced to Rudnick and Gao (2003), similarly hereinafter.

and leuconorite with sharp contacts and also in melanorites with gradational contacts (Chen et al., 2015b). Magnetites from two Fe-Ti-P ores have obviously different Ge contents, with Ge ranges from 1.36 to 4.48 ppm and from 14.8 to 26.6 ppm (Fig. 1a) (Liu et al., 2015). The high-Ge magnetite has higher Zn and Ga contents, but lower Cr, Co and Ni contents. Both Cr contents and Co/Ni ratios are considered to be mainly related to fluids derived from variable magmas (Carew, 2004; Dare et al., 2014), and thus these values are used to discriminate magnetite from hydrothermal deposits and BIFs (Chen et al., 2015c). In magmatic system, different Cr and Ni contents of magnetite from different ores may be related to different degrees of evolution of magma or different nature of the magmas (e.g., mafic rocks or granitoids) (Dare et al., 2014; Nadoll et al., 2014; Chen et al., 2015c). Therefore, different Ge contents in magnetite from the same deposit may be due to the degree of magmatic evolution. During crystal fractionation, late magnetite may be depleted in compatible elements such as Cr, Co, Ni but be enriched in moderately incompatible elements such as Ge, Ga and Zn relative to early magnetite.

(3) Ni-Cu-PGE deposits

Magnetite is a common accessory mineral in magmatic Ni–Cu–PGE sulfide deposits, which forms in those

associated with mafic and intermediate rocks, such as the Sudbury Igneous Complex in Canada (Hawley and Stanton, 1962), Voisey's Bay Anorthosite Complex in Canada (Naldrett et al., 2000), Noril'sk-Talanakh intrusion in Siberia (Czamanske et al., 1992), and Huangshandong intrusion in China (Zhou et al., 2004; Gao et al., 2013). Magnetite (also titanomagnetite) in massive sulfides of Sudbury Ni–Cu–PGE deposits contains 0.15–1.27 ppm Ge with the average content of 0.74 ppm (Fig. 1a) (Dare et al., 2012). In a sulfide melt, Ge together with other lithophile elements such as Cr, Ti, V, Al, Mn, Ga are compatible into Iron oxides so that Ge contents in Iron oxides gradually decrease with the continual crystallization of Fe-oxide from the sulfide liquid (Dare et al., 2012). For example, Ge contents in magnetite or titanomagnetite of Sudbury crystallized from primitive Fe-rich monosulfide solution (MSS), evolved Fe-rich MSS, and residual Cu-rich intermediate solid solution (ISS) are 0.61–1.27 ppm (average 1.03 ppm), 0.29–0.92 ppm (average 0.44 ppm), and 0.15–0.37 ppm (average 0.22 ppm), respectively, showing a decreasing trend (Dare et al., 2012). The positive correlation between Ge and Cr also indicates the compatibility of Ge in magnetite (Dare et al., 2012). This behavior of Ge in magnetite from sulfide liquid is in contrast with Fe-oxides that crystallized from a fractionating silicate melt, whereby the concentration of incompatible elements, such as Ti, increases rather than decreases (Dare et al., 2012).

The Permian Huangshandong intrusion, the largest in the eastern Tianshan orogenic belt of NW China, hosts significant Ni-Cu sulfide mineralization. Oxide-bearing sulfide mineralization contains 1vol% to 5vol% magmatic magnetite that has ilmenite and spinel exsolution lamellae (Gao et al., 2013). Magnetite contains variable amounts of Mg, Ti, Al, Cr, V, Zn and Sn, indicating that they crystallized from different stages during magma differentiation (Gao et al., 2013). Magnetite contains 0.1–8.3 ppm Ge with an average of 0.9 ppm (Fig. 1a) (Gao et al., 2013), similar to the Ge content of magnetite from the Sudbury deposit.

3.1.2 Iron formations

Iron formations are economically important sedimentary rocks that are most common in Precambrian sedimentary successions. Texturally, iron formations were also divided into banded iron formation (BIF) and granular iron formation (GIF). BIF is dominant in Archean to earliest Paleoproterozoic successions, whereas GIF is mainly distrubuted in Paleoproterozoic successions (Bekker et al., 2010). Precambrian BIFs are alternating layers of iron-rich and silica-rich chemical precipitates, which are important indicators for the environmental change and geochemical evolution of the early Earth (Klein, 2005). The Sokoman Iron Formation in the Labrador Trough of Canada is a typical GIF, coeval with the ~1.88 Ga Nimish volcanic suites in the same region. There are three occurrences of magnetite, including primary and altered magnetite in iron formations and magnetite in volcanic breccia associated with the iron formation (Chung et al., 2015). These three types of magnetite have different trace elemental compositions. Primary magnetite has a relatively narrow range of composition with the depletion of Ti, Pb, Mg and Al, whereas magnetite in volcanic breccia is rich in Ti, Al, V, Mn, Mg, Zn, Cu and Pb. Altered magnetite shows a relatively wide range of trace elemental composition that overlapped the range of primary magnetite. Primary magnetite contains 13–39 ppm Ge with an average Ge content of 23 ppm, whereas altered magnetite contains 3.8–110 ppm Ge with an average content of 25 ppm (Fig. 1b) (Chung et al., 2015). Magnetite in volcanic breccia has Ge content ranging from 12.1 to 247 ppm and the average Ge content of 59 ppm (Fig. 1b) (Chung et al., 2015). The wide range of Ge in altered magnetite may indicate the variable degree of hydrothermal modification or modification by highly various fluid compositions, likely related to volcanism.

Magnetite from banded magnetite-chert-feldsparbiotite of Pipe mine, Thompson Ni belt, Canada has an average Ge content of 11.2 ppm (Fig. 1b) (Dare et al., 2014), similar to the content lower limit of those from the Sokoman iron formation.

3.1.3 Skarn Fe deposits

The Mesozoic Tengtie skarn Fe deposit in the Nanling Range, South China is contemporaneous with the regional Sn mineralization. The deposit is composed of numerous ore bodies along the contacts between the late Paleozoic or Mesozoic carbonate rocks and the Yanshanian Lianyang granitic complex. The Tengtie deposit has a paragenetic sequence of the prograde stage of anhydrous skarn minerals, followed by the retrograde stage of hydrous skarn minerals, and the final sulfide stage (Zhao and Zhou, 2015). Magnetite from three stages has similar Ge content ranging from 0.2 to 5.8 ppm with an average content of 1.1 ppm (Fig. 1c) (Zhao and Zhou, 2015).

The Fenghuangshan Cu–Fe–Au deposit in the Tongling of Eastern China is a typical skarn deposit (Yin Jiangning et al., 2016). The deposit has a paragenetic sequence of the prograde skarn stage, followed by the retrograde skarn stage, and the final quartz-sulfide and carbonate stages. Magnetite mainly occurs in retrograde and carbonate stages. Magnetite from this deposit contains 1.5–73 ppm Ge with an average Ge content of 11 ppm (Fig. 1c)

(Huang et al., 2016).

Magnetite from the retrograde exoskarn of calcic skarn Fe deposit in Vegas Peledas of Argentina has an average Ge content of 2 ppm (Dare et al., 2014), similar to those of magnetite from other skarn deposits.

3.1.4 Iron Oxide Copper–Gold (IOCG) deposits

IOCG deposit is one of the most important iron deposit types (Liu shaofeng and Fu Shuxing, 2016). Numerous giant Fe-Cu deposits such as Lala, Dahongshan, and Yinachang deposits are distributed in the Kangdian IOCG metallogenic province of SW China (Zhao and Zhou, 2011; Zhao et al., 2013). These deposits have a common paragenetic sequence of an early Fe-oxide stage associated with sodic alteration and a late Cu-sulfide stage associated with potassic carbonate alteration. Magnetite occurs mainly in the Fe-oxide stage of these deposits but is also present in the Cu-sulfide stage of the Lala deposit. Magnetite from the oxide stage of Lala deposit contains 1.1–5.1 ppm Ge (average 3 ppm), whereas those from the sulfide stage of Lala deposit contain similar Ge contents of 0.6–4.0 ppm (average 2.3 ppm) (Fig. 1d) (Chen et al., 2015a). This indicates associated minerals may have little effect on the Ge partition into magnetite. Magnetite from the Dahongshan deposit contains 0.8–5.5 ppm Ge with an average content of 3.1 ppm (Fig. 1d) (Chen et al., 2015a). Those from the Yinachang deposit have Ge contents ranging from 0.9 to 1.4 ppm with an average content of 1.3 ppm (Fig. 1d) (Chen et al., 2015a). The lower V and Ni but higher Sn and Mo contents of magnetite from the Yinachang deposit are thought to have precipitated from more oxidized and Mo-Sn-rich fluids that may have evolved from relatively felsic magmas (Chen et al., 2015a). Therefore, the higher Ge contents in magnetite from the Lala and Dahongshan deposits than those of magnetite from the Yinachang deposit may reflect different fluid composition.

The Ernest Henry deposit in the Cloncurry district of Australia is a typical IOCG deposit, the scale of which is second only to Olympic Dam. Ores are hosted in a structurally controlled hydrothermal breccia vein or pipe-like body that has gradational contacts with a crackle breccia (Mark et al., 2006). The ores are composed of rounded clasts of potassically altered metavolcanics and a matrix dominated by magnetite, pyrite, chalcopyrite, calcite, and quartz with minor apatite, actinolite, fluorite, barite, and biotite (Mark et al., 2006). Magnetite from the ores contains 0.61–0.89 ppm Ge with an average content of 0.72 ppm (Fig. 1d) (Dare et al., 2014).

3.1.5 Igneous derived hydrothermal Fe deposits

The Cihai Fe deposit in the Beishan terrane of NW China is a diabase-hosted magmatic hydrothermal deposit. Ore minerals are dominantly magnetite, pyrite, and pyrrhotite, with minor chalcopyrite, galena, and sphalerite. Gangue minerals include pyroxene, garnet, hornblende and minor plagioclase, biotite, chlorite, epidotite, quartz, and calcite. Re–Os age of pyrite and the composition of magnetite indicate that the Cihai Fe deposit may have derived from magmatic–hydrothermal fluids related to mafic magmatism (Huang et al., 2013b). Magnetite from the Cihai deposit contains 0.26–3.6 ppm Ge with an average Ge content of 0.76 ppm (Fig. 1e) (Huang et al., 2013b).

Heifengshan, Shuangfengshan, and Shaquanzi Fe deposits in the Eastern Tianshan Orogenic Belt of NW China are hosted in Carboniferous volcanic rocks and share a common mineral assemblage of magnetite, pyrite, calcite, and chlorite (Wang Tianfeng et al., 2016). These deposits are considered to have formed from magmatic hydrothermal fluids (Huang et al., 2013a; Huang Xiaowen et al., 2014b). Magnetite from the Heifengshan, Shuangfengshan and Shaquanzi deposits have Ge contents of 0.03–0.68 ppm (average 0.17 ppm), 0.03–2.08 ppm (average 0.3 ppm), and 0.2–2.02 ppm (average 0.54 ppm), respectively (Fig. 1e) (Huang Xiaowen et al., 2014a). Many magnetite grains have Ge contents lower than the detection limits.

3.2 Controlling factors of Ge in magnetite

In general, magnetite from different types of deposits has various trace element compositions (Fig. 2). The average Ge content of magnetite, from high to low, has the sequence of iron formations, skarn Fe deposits, IOCG deposits, magmatic Fe deposits, magmatic sulfide deposit, and igneous derived hydrothermal Fe deposits (Fig. 2). This indicates that Ge contents of magnetite from different deposit types may be controlled by different factors. The concentration of Ge in magmatic/hydrothermal magnetite may depend on (a) the concentration of Ge in the primary magma/fluids from which it crystallizes, (b) partition coefficient of Ge into magnetite, and (c) physicochemical conditions (temperature, oxygen fugacity and sulfur fugacity) (e.g., Dare et al., 2014; Nadoll et al., 2014).

3.2.1 Primary magma/fluids

Fe-Ti-(V) deposits commonly form from evolved silicate melt (~ferrodiorite in composition) at the top of layered intrusions. Intrusions of Bushveld Complex and Sept Iles are associated with plume-related magmas in a rift environment (Higgins, 2005; Barnes et al., 2010). Fe-Ti-(V) deposits in ELIP are considered to be related to high-Ti picritic magmas derived from the Emeishan mantle plume (Zhou et al., 2013; Wang et al., 2014). The parental magmas for the mafic–ultramafic intrusions in the ELIP may have evolved from the high-Ti picritic magmas.

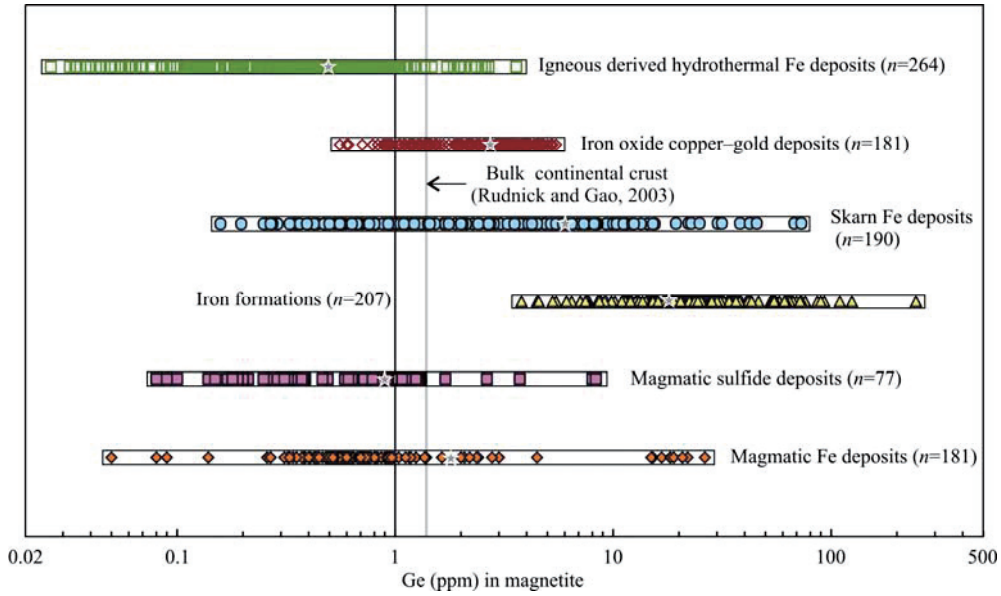

Fig. 2. Summary of Ge concentrations of magnetite from various types of iron deposits and sulfide deposits.
"*n*" in parentheses represents the number of data. Data sources are the same as Fig.1.

Ni-Cu-PGE deposits such as Sudbury are suggested to derive from the andesitic liquid which formed by flash-melting the continental crust (Ames et al., 2002). Because primitive mantle, oceanic crust, and continental crust have similar Ge contents of 1.1 ppm, 1.5 ppm and 1.6 ppm, respectively. Melting of mantle or crust or both would produce magmas with similar Ge contents. But the composition of primary magma may be different due to mantle heterogeneities. Moreover, Ge becomes progressively enriched in the final products of crystallization of the alkali lava series (De Argollo and Schilling, 1978). However, Ge/Si ratios are considered independent of degree of partial melting and extent of fractional crystallization effective in the generation of basaltic lavas and thus Ge/Si ratio in basalts may be a useful mantle source indicator and should help mapping mantle heterogeneities (De Argollo and Schilling, 1978). For magnetite formed from silicate melts, Ge is compatible but Si is extremely incompatible in magnetite (see summary of partition coefficient of trace elements in magnetite by Dare et al., 2012), and thus Ge/Si ratios of magnetite will increase with the increasing fractional crystallization. The positive correlation between Ge and Ge/Si ratios for magnetite from Anyi and Baima intrusions indicates that Ge/Si ratios of magnetite from these two intrusions may have been affected by fractional crystallization (Fig. 3). This is consistent with more various trace element contents of magnetite from Baima and Anyi (Liu et al., 2015). Different Ge/Si ratios of magnetite from intrusions in ELIP may also reflect heterogeneous mantle sources from which primary magma

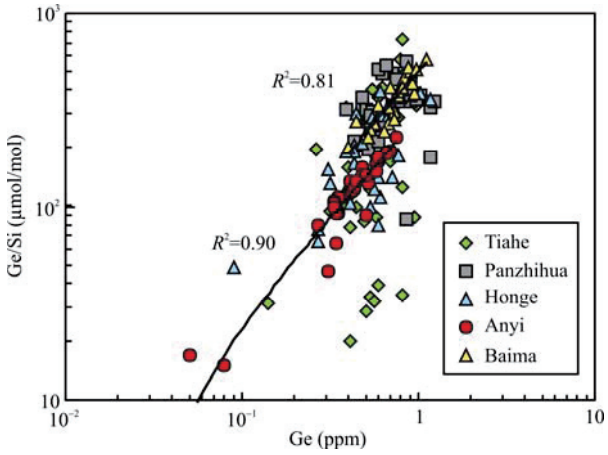

Fig. 3. Plot of Ge concentration versus Ge/Si ratio (expressed as μmol/mol) for magnetite from intrusions of Emeishan large igneous province. Data sources are the same as Fig.1.

produced. Magnetite from those Fe-Ti-P deposits has obviously higher Ge content than those from Fe-Ti-V deposits and Ni-Cu-PGE deposits (Fig. 1), which are possible due to the various magma compositions/ formation mechanisms (Liu et al., 2015).

There are rare Ge data of magnetite in igneous rocks. Dare et al. (2014) reported that magnetite from fresh calc alkaline lavas in Lascar and El Laco stratovolcanoes, northern Chile contain 0.4–0.6 ppm Ge with an average Ge content of 0.5 ppm. Assuming that Ge content in silicate melts is equal to that of average continental crust, the calculated partition coefficient between magnetite and silicate melt is about 0.4, which is slightly higher than the

low partition coefficient (0.11) between spinel and silicate melt (Malvin and Drake, 1987). Magnetite from the magmatic Fe-Ti-V deposits also has Ge contents mostly less than 1 ppm (Fig. 1). The relatively depletion of Ge in magmatic magnetite indicates differentiation of a silicate melt did not enrich Ge in magnetite. However, Ge is compatible into magnetite in a sulfide melt and thus magnetite crystallizing first has the highest Ge content (Dare et al., 2012). Therefore, fractionation crystallization of silicate magma would enrich Ge in residual magma, whereas fractionation crystallization of sulfide melt would enrich Ge in magnetite.

Germanium behavior in hydrothermal system has been widely studied (Arnórsson, 1984; Mortlock et al., 1993; Pokrovski and Schott, 1998; Wheat and McManus, 2008). Germanium in hydrothermal fluids is probably derived from two major sources (Bernstein, 1985). Germanium may be concentrated in the evolved magmatic hydrothermal fluids through fractional crystallization or be picked up from the country rocks, particularly from organic-bearing rocks, by migrating fluids. Ge in geothermal systems is considered to be controlled by exchange reactions where it substitutes for silica in silicates and iron in sulfides (Arnórsson, 1984). It is the rate of dissolution, water Ph and the proportion of the alteration minerals which take up Ge to a variable extent that ultimately fix Ge concentration in the water (Arnórsson, 1984). Germanium in mid-ocean ridge hydrothermal fluids is controlled by seawater-basalt reactions (Mortlock et al., 1993; Wheat and McManus, 2008). Experimental studies have showed that the partition coefficient of Ge between aqueous fluids and coexisting granitic melts is 0.0003–0.06 (Bai and van Groos, 1999). Germanium tends to partition into melt phases during pneumatolytic hydrothermal process. However, some studies have showed that Ge is commonly concentrated in some minerals of granitic pegmatites and greisens, particularly topaz, micas and spodumene (Bernstein, 1985). The Ge contents generally increase during fractionation of granitic melts and Ge is enriched and hosted in newly formed hydrothermal topaz during greisenization (Breiter et al., 2013). The relative enrichment of Ge in these hydrothermal minerals is possibly due to the substation of Al^{3+} by Ge^{4+} or related to the low extent of polymerization of these minerals (Tu Guangchi, 2004).

Therefore, for most magmatic hydrothermal deposits absent of organic material, the composition of magma-related hydrothermal fluids and the degree of fluid-rock reaction are the main factors controlling the Ge in ore-forming fluids from which magnetite formed.

3.2.2 Physicochemical conditions

Temperature, oxygen fugacity and sulfur fugacity are important controlling factors of trace elements in magnetite. Oxygen fugacity within a melt is the major control on element partitioning between oxides, and between oxides and silicates at magmatic temperatures (Frost and Lindsley, 1991). Many studies have focused on dependence of Ge partitioning behavior between coexisting solid metal and liquid silicate phases on oxygen fugacity, temperature and melt composition under terrestrial core formation condition (e.g., Capobianco et al., 1999; Kegler and Holzheid, 2011; Righter et al., 2011). However, the dependence of Ge partitioning between silicate/sulfide melt and magnetite on physicochemical conditions is rarely reported. There are two geologically relevant Ge compounds, GeS_2 and GeO_2, which are stable at different temperatures, oxygen and sulfur fugacities (Fig. 4). Within the fO_2 range of −0.9 to −2.7 log units relative to the Fe-FeO (IW) buffer, the valence state of Ge is 2.00 (±0.12), i.e. GeO is the stable species in the silicate melt, which is in good agreement with the results acquired at 1 atm, 1300 °C and a comparable fO_2 range of −0.5 to −2.7 log units relative to the IW buffer (Kegler and Holzheid, 2011). But tetravalent Ge (GeO_2) is stable in silicate melts at 1 atm and more oxidizing conditions (−1.3 to +3.8 log units relative to IW buffer) (Kegler and Holzheid, 2011). The stable field of GeO_2 commonly overlaps that of magnetite (Fig. 4), indicating that tetravalent Ge is relatively stable in magnetite. Therefore, relatively high oxygen fugacity is possibly beneficial for Ge partition into magnetite.

In sulfide-dominated environments sulfur fugacity can be the primary control for the partitioning behavior of relevant elements (Dare et al., 2012). For magnetite crystallizing from sulfide melts, Ge shows similar behaviors with lithophile elements, Cr, Ti and V, indicating that these elements partition into Fe-oxide, rather than sulfide phases (Dare et al., 2012). Therefore, sulfur fugacity possibly has little effect on Ge partition into magnetite.

Partition coefficients are greatly temperature dependent (McIntire, 1963). There is a trend that cooler temperature hydrothermal magnetite generally has lesser trace element concentrations, whereas high-temperature hydrothermal porphyry and skarn magnetite shows relatively higher minor and trace element concentrations (Nadoll et al., 2014). Positive correlation between germanium content of the water and its temperature indicates that temperature is critical for Ge enrichment in geothermal systems (Arnórsson, 1984). Total concentrations of Ti and V are considered to be indicator of temperature of magnetite (Nadoll et al., 2014). However, there is no obvious correlation between Ge in magnetite and crystallization temperature (Fig. 5). Low temperature magnetite from BIF

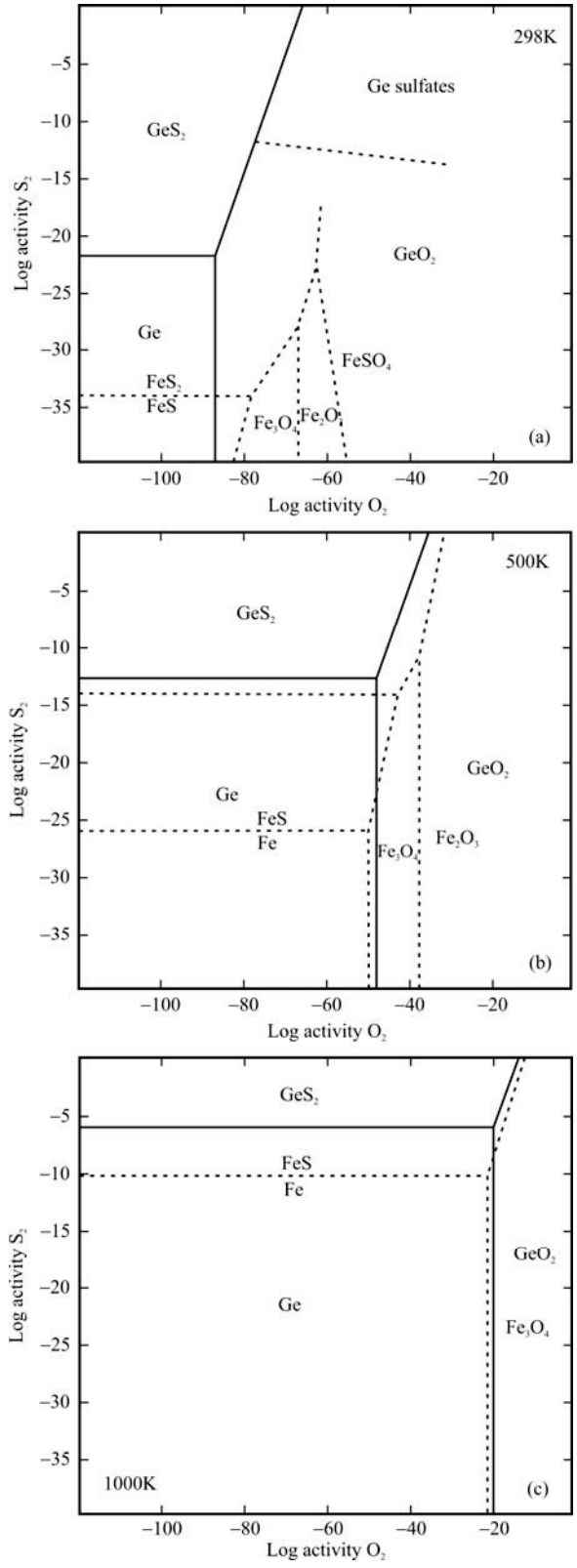

Fig. 4. The stable fields of Ge, GeS_2, GeO_2, and Fe compounds as related to the activities of O_2 and S_2 at 298, 500, and 1000 K and 1 atmosphere (Bernstein, 1985).

has the highest Ge contents. Moreover, magnetite from volcanic breccias in granular iron formations also has high Ge contents (Chung et al., 2015). Exsolution lamellae of ilmenite is observed in the magnetite, which are possibly the result of a volcanic input of pyroclastic origin during or shortly after deposition (Chung et al., 2015). Therefore, temperature is not the key factor for Ge in magnetite. The special formation mechanism of magnetite in BIF is the major governing factor which will be discussed in the following part.

3.3 Ge enrichment in magnetite of iron formations

Magnetite from the banded/granular iron formations has the highest Ge contents relative to other types of iron deposits (Fig. 2). The Ge contents of magnetite in iron formations are commonly 10 or even 100 times that of bulk continental crust. This indicates that Ge enrichment in magnetite of BIFs is probably due to the special formation environment and mechanism of magnetite.

The common fine lamination (and/or microbanding) as well as the lack of detrital components in most BIFs was considered to chemical deposition below wave base, in the deeper parts of ocean basins (Klein, 2005). Those with granular textures are regarded as the result of deposition in shallow platformal areas (Klein, 2005). The origin of iron formation is complex and remains a matter of controversy (Bekker et al., 2010). Iron and Si in BIFs were considered to originally derived from deep-sea hydrothermal fluids admixed with sea water and were precipitated under anoxic conditions (Klein, 2005).

It was suggested that the enrichment of Ge in sedimentary iron deposits and in the oxidized zones of iron-bearing sulfide deposits is probably due to incorporate Ge to iron hydroxides when they are precipitated from aqueous solutions (Bernstein, 1985). This deduction was based on the fact that 93%–95% of dissolved Ge to be precipitated by $Fe(OH)_3$ from sea water with a pH greater than about 6 (Burton et al., 1959; Pazenkova, 1967). Experimental study also demonstrates that Ge is likely to be absorpted by or coprecipitated with iron hydroxides and organo-mineral colloids in many superficial aquatic environments at the contact of anoxic groundwaters with surficial oxygenated solutions (Pokrovsky et al., 2006). Some studies also conclude that "missing Ge sink" in ocean is due to Ge sequestration into authigenic Fe-oxyhydroxides in marine sediments (Escoube et al., 2015). However, Ge/Si ratios of iron formations indicate that silica is dominantly derived from weathering of continental landmass, whereas iron has a hydrothermal origin (Hamade et al., 2003). Moreover, recent studies have demonstrated that Ge sequestration by Fe-oxyhydroxides might not be the major factor that

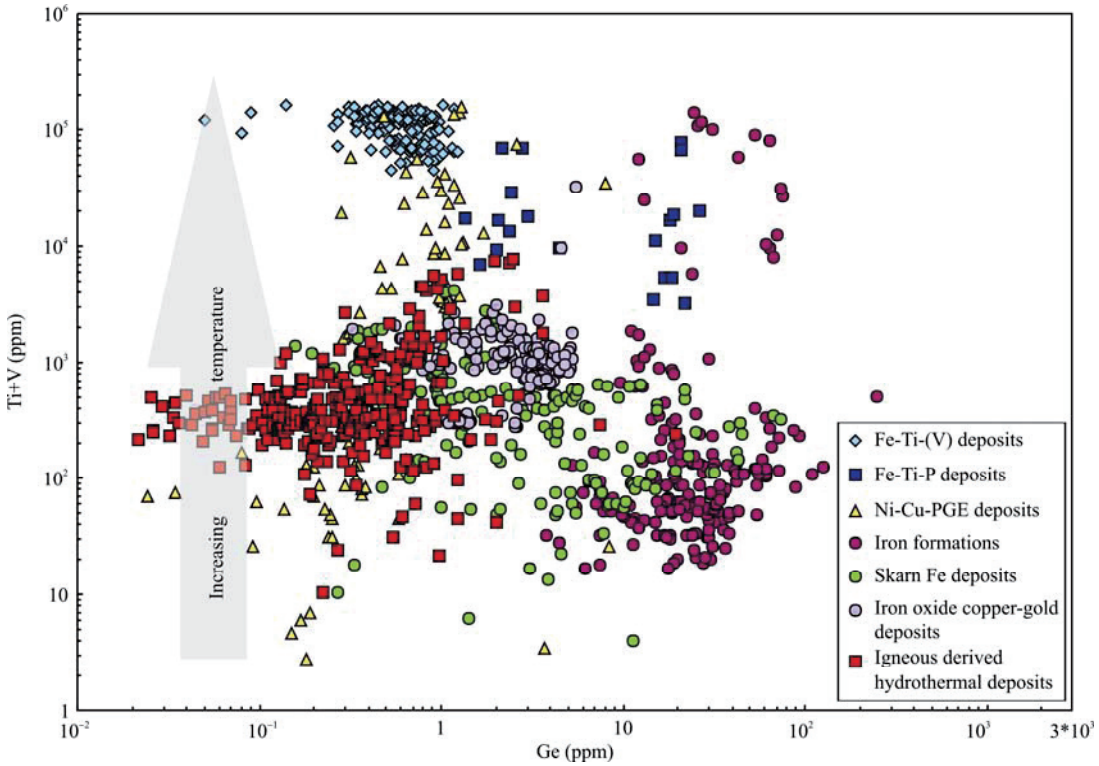

Fig. 5. Plot of Ge verus Ti+V for magnetite from different type of deposits. Total Ti and V concentration was used as a temperature indicator.

controls the differences in Ge/Si ratios between Si-rich and Fe-rich layer (Delvigne et al., 2012). Therefore, Ge enrichment in iron formation remains unknown and needs further study.

4 Potential Application of Ge in Magnetite

4.1 Ge in magnetite as a discriminate factor

Trace elements in magnetite could be very useful for discriminating deposit types (Yi Liwen et al., 2015). For example, Dupuis and Beaudoin (2011) suggested that the Ni+Cr vs. Si+Mg diagram is efficient in separating magnetite from Ni-Cu sulfide deposits from the magnetite and/or hematite from all other deposit types. However, recent studies have found that magnetite from Ni-Cu deposits has more various compositions than previously thought (Liu et al., 2015). The plot of Ni+Cr vs. Si+Mg, thus, cannot separate Ni-Cu deposits from others and cannot discriminate different types of magmatic deposits. Plot of Ge vs. Ga+Co was proposed to differentiate magnetite of Fe–Ti–(V) oxide-bearing layered intrusions in the ELIP from that of massif anorthosites and magmatic Cu–Ni sulfide deposits (Liu et al., 2015). Chen et al., (2015c) proposed that the plot of Ti/Al versus Ge can separate the BIF-type magnetite from the magnetite of the sheared magnetite-quartzites and other types of ores from the Cu-(Au, Fe) deposits in the Khetri copper belt of NW India.

There are no obvious differences in Mg and Al contents of magnetite from all types of deposits (Figs. 6a and b). Magmatic Fe-Ti-(V) and Fe-Ti-P deposits define different fields due to higher Ti, V and Cr contents (Figs. 6c–e). Different types of hydrothermal deposits define different fields in the plot of Mn versus Ge (Fig. 6f). There are no obviously different Co contents of magnetite from different types of deposits (Fig. 6g). In the plot of Ge versus Ni (Fig. 6h), magnetite from magmatic deposits, hydrothermal deposits and sedimentary deposits defines different fields, so that this plot can be used to distinguish these deposit types. Magnetite from the iron formations has lower Zn and higher Ge than those from other deposits (Fig. 6i). Magnetite from the magmatic (-hydrothermal) Fe deposits, magmatic sulfide deposits and sedimentary deposits has different Ga and Ge contents (Fig. 6j). This trend is more obvious in the plot of Ge versus Ge/Ga in spite of partial overlapping (Fig. 7a). In the plot of Ge vs. Ge/Si, magnetite from the magmatic hydrothermal deposits has higher Ge/Si ratios than those from other deposits (Fig. 7b). From what has been discussed above, we can conclude that Ge together with other elements and some element ratios have the potential to discriminate deposit types or mineralization types. This has important implications for the application of Ge as a discriminate factor like Ti and V to reveal the ore genesis of different types of magnetite-bearing deposits.

4.2 Ge/Si ratio of magnetite as a geochemical tracer

The geochemical behavior of inorganic Ge in low-temperature processes is analogous to that expected for a superheavy stable isotope of Si (Mortlock and Froelich, 1987; Mortlock et al., 1993). Inorganic Ge exists as the same chemical species as Si in natural waters due to their similar atomic radii and Si-O, Ge-O bond lengths and can substitutes for Si in the SiO_2 lattice (Pokrovski and Schott, 1998). Ge/Si ratios have been used to discuss the genesis of banded iron formations because the Ge/Si ratio preserved in iron formation silica should reflect the ratio of the water from which it precipitated and hence reflect its source (e.g., Hamade et al., 2003; Delvigne et al., 2012; Escoube et al., 2015). Previous studies mainly focus on the Ge/Si ratios of Fe-rich layers and Si-rich layers such as chert. These ratios are commonly obtained by chemical analytical method

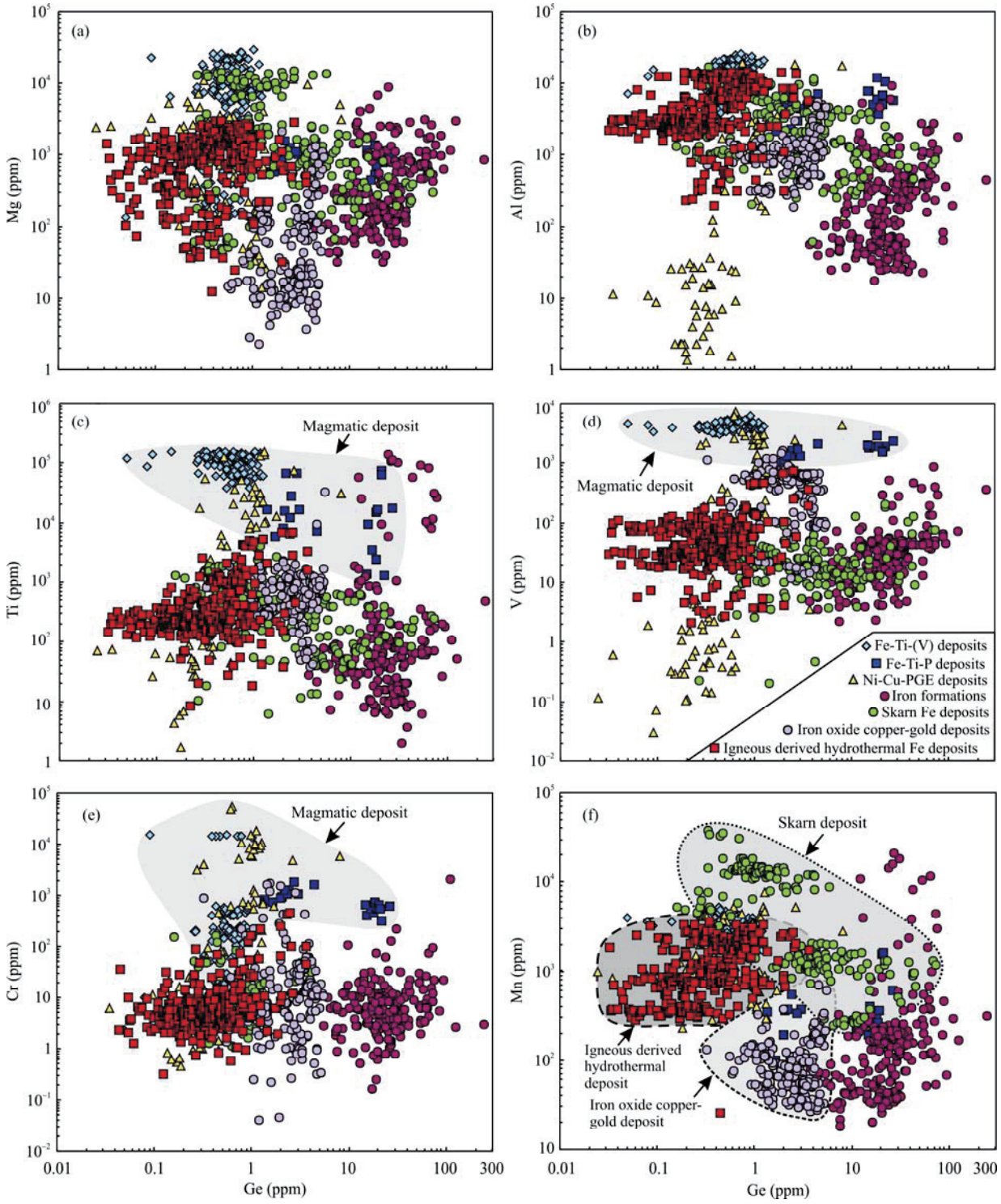

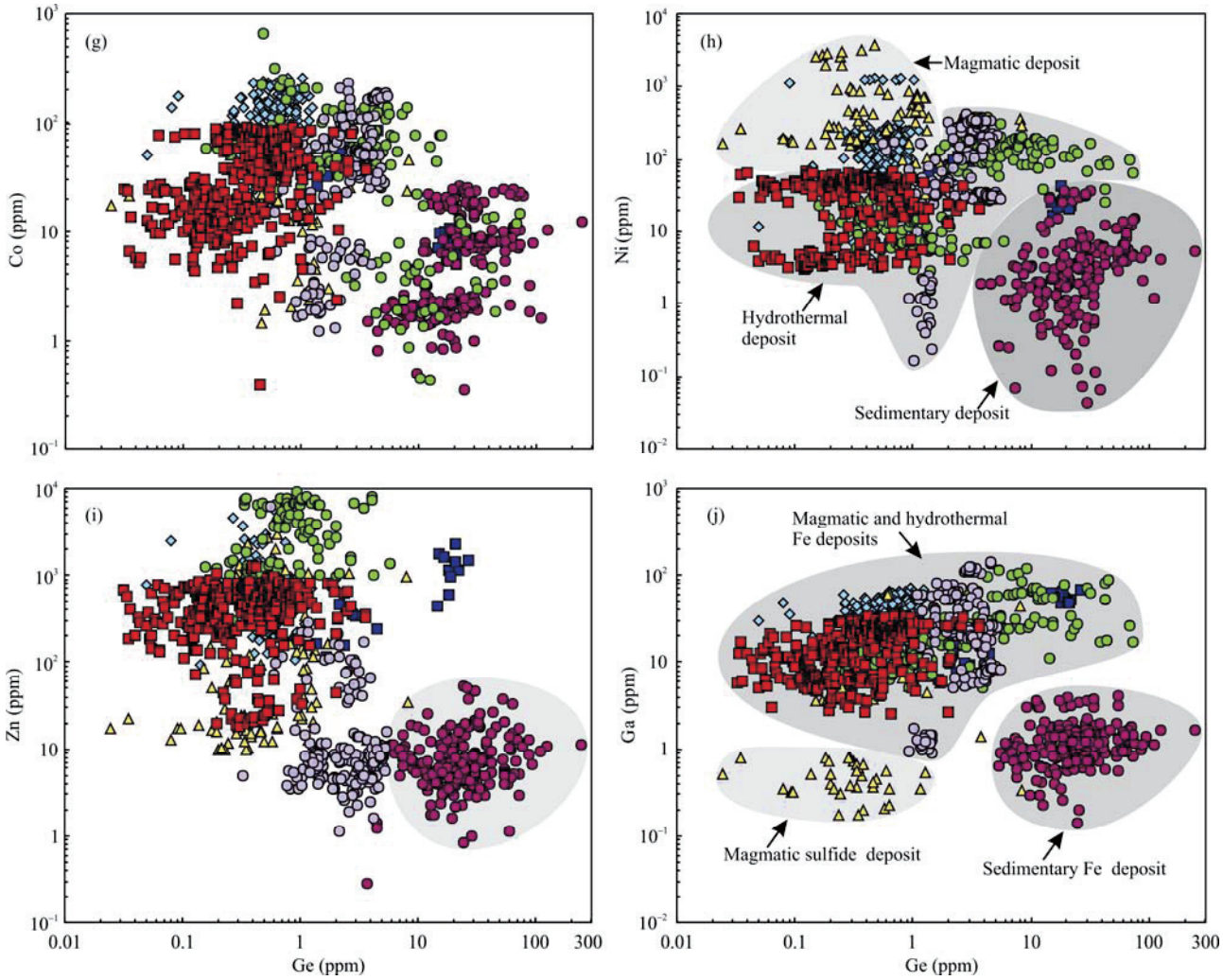

Fig. 6. Plots of Ge versus Mg, Al, Ti, V, Cr, Mn, Co, Ni, Zn, and Ga showing the different chemical compositions of magnetite from different types of deposits.

which is unavoidably affected by contamination of other mineral inclusions. Moreover, different stages or generations of magnetite cannot be distinguished, limiting the application of Ge/Si ratios. With the development of in situ LA-ICP-MS trace element analysis of magnetite, we can obtain in situ Ge/Si ratios of magnetite, particularly these with complex textures and multiple generations. Thus, in situ Ge/Si ratio of magnetite can serve as a geochemical tracer and may offer new constraints on the genesis debate of banded iron formations.

5 Conclusions

Germanium is a typical dispersed element in the earth but sometimes is not depleted in magnetite. Numerous in situ LA-ICP-MS trace element data of magnetite from different types of deposits are summarized with an emphasis on Ge geochemistry of magnetite. Germanium was mainly enriched in magnetite from banded iron formations with Ge contents ranging from 10 to ~250 ppm. Magnetite from the magmatic Fe/sulfide deposits, skarn Fe deposits, iron oxide copper-gold deposits, and igneous derived hydrothermal deposits has the similar Ge contents mostly less than 10 ppm. Germanium in magnetite from magmatic/hydrothermal deposits was controlled by some factors. Primary magma/fluid composition may be the major control of Ge in magnetite and higher oxygen fugacity may be beneficial to Ge partition into magnetite. Sulfur fugacity and temperature may have little effect on Ge in magnetite. Germanium enrichment mechanism in magnetite of iron formations remains unknown due to its genetic complexity and thus this aspect needs further study. Plots of Ge versus other elements and element ratios can be used to distinguishing deposit types, indicating that Ge can serve as a discriminate factor like Ti and V in magnetite. Due to the development of in situ trace element analytical technique, in situ Ge/Si ratio of magnetite can be used as a

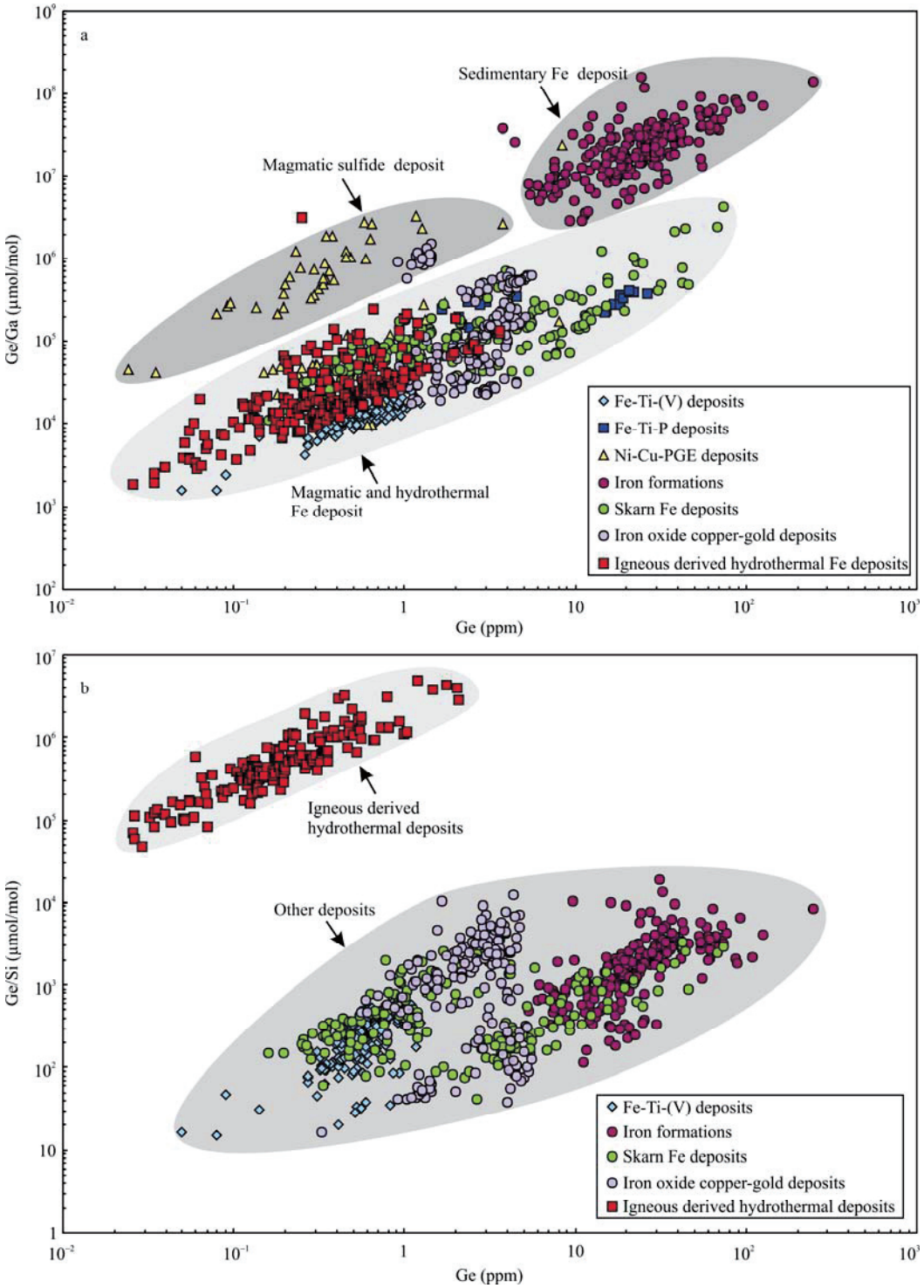

Fig. 7. Plots of Ge verus Ge/Ga (a) and Ge versus Ge/Si (b) for magnetite from different types of deposits. Magnetite from the magmatic and hydrothermal deposits has lower Ge/Ga ratios than those from the magmatic sulfide deposits and sedimentary deposits. Magnetite from the igneous derived hydrothermal deposits has Ge/Si ratios higher than other deposits.

geochemical tracer and provide new constraints on the genesis of banded iron formations.

Acknowledgements

This study was funded by CAS "Light of West China" Program to YMM, the Key project of the National Natural Science Foundation of China (41230316), National Natural Science Foundation of China (41503039), the "CAS Hundred Talents" Project to JFG (Y5CJ038000), Research Initial Funding (Y4KJA20001 and Y5KJA20001) and Independent Topics Fund

(Y4CJ009000) of the Institute of Geochemistry, Chinese Academy of Sciences. We thank construction comments from anonymous reviewers.

Manuscript received May 29, 2016
accepted Nov. 20, 2016
edited by Liu Lian

References

Ames, D.E., Golightly, J.P., Lightofot, P.C., and Gibson, H.L., 2002. Vitric Compositions in the Onaping Formation and their Relationship to the Sudbury Igneous Complex, Sudbury Structure. *Economic Geology*, 97(7): 1541–1562.

Arnórsson, S., 1984. Germanium in Icelandic geothermal systems. *Geochimica et Cosmochimica Acta*, 48(12): 2489–2502.

Bai, T.B., and van Groos, A.F.K., 1999. The distribution of Na, K, Rb, Sr, Al, Ge, Cu, W, Mo, La, and Ce between granitic melts and coexisting aqueous fluids. *Geochimica et Cosmochimica Acta*, 63(7–8): 1117–1131.

Barnes, S., Maier, W.D., and Curl, E.A., 2010. Composition of the marginal rocks and sills of the Rustenburg Layered Suite, Bushveld Complex, South Africa: implications for the formation of the platinum-group element deposits. *Economic Geology*, 105(8): 1491–1511.

Bekker, A., Slack, J.F., Planavsky, N., Krapež, B., Hofmann, A., Konhauser, K.O., and Rouxel, O.J., 2010. Iron formation: the sedimentary product of a complex interplay among mantle, tectonic, oceanic, and biospheric processes. *Economic Geology*, 105(3): 467–508.

Bekmukhametov, A.E., Zamyatina, G.M., and Kalinin, S.K., 1973. Geochemistry of germanium in the iron deposits of Kazakhstan. *Geochemistry International*, 5: 277–282.

Belissont, R., Boiron, M.C., Luais, B., and Cathelineau, M., 2014. LA-ICP-MS analyses of minor and trace elements and bulk Ge isotopes in zoned Ge-rich sphalerites from the Noailhac-Saint-Salvy deposit (France): Insights into incorporation mechanisms and ore deposition processes. *Geochimica et Cosmochimica Acta*, 126: 518–540.

Bernstein, L.R., 1985. Germanium geochemistry and mineralogy. *Geochimica et Cosmochimica Acta*, 49(11): 2409–2422.

Breiter, K., Gardenová, N., Kanický, V., and Vaculovič, T., 2013. Gallium and germanium geochemistry during magmatic fractionation and post-magmatic alteration in different types of granitoids: a case study from the Bohemian Massif (Czech Republic). *Geologica Carpathica*, 64(3): 171–180.

Burton, J.D., Culkin, F., and Riley, J.P., 1959. The abundances of gallium and germanium in terrestrial materials. *Geochimica et Cosmochimica Acta*, 16(1): 151–180.

Capobianco, C.J., Drake, M.J., and De'Aro, J., 1999. Siderophile geochemistry of Ga, Ge, and Sn: cationic oxidation states in silicate melts and the effect of composition in iron-nickel alloys - The effects of pressure, temperature, oxygen fugacity, and silicate and metallic melt compositions. *Geochimica et Cosmochimica Acta*, 63(17): 2667–2677.

Carew, M.J., 2004. *Controls on Cu-Au mineralisation and Fe oxide metasomatism in the Eastern Fold Belt, NW Queensland, Australia.* Queensland: James Cook University (Ph.D thesis): 213–277.

Chen, W.T., Zhou, M.F., Gao, J.F., and Hu, R., 2015a. Geochemistry of magnetite from Proterozoic Fe-Cu deposits in the Kangdian metallogenic province, SW China. *Mineralium Deposita,* 50(7): 795–809.

Chen, W.T., Zhou, M.F., Gao, J.F., and Zhao, T.P., 2015b. Oscillatory Sr isotopic signature in plagioclase megacrysts from the Damiao anorthosite complex, North China: Implication for petrogenesis of massif-type anorthosite. *Chemical Geology*, 393: 1–15.

Chen, W.T., Zhou, M.F., Li, X., Gao, J.F., and Hou, K., 2015c. In-situ LA-ICP-MS trace elemental analyses of magnetite: Cu-(Au, Fe) deposits in the Khetri copper belt in Rajasthan province, NW India. *Ore Geology Reviews*, 65: 929–939.

Chung, D., Zhou, M.F., Gao, J.F., and Chen, W.T., 2015. In-situ LA-ICP-MS trace elemental analyses of magnetite: The late Palaeoproterozoic Sokoman Iron Formation in the Labrador Trough, Canada. *Ore Geology Reviews*, 65: 917–928.

Cook, N.J., Etschmann, B., Ciobanu, C.L., Geraki, K., Howard, D.L., Williams, T., Rae, N., Pring, A., Chen, G., and Johannessen, B., 2015. Distribution and Substitution Mechanism of Ge in a Ge-(Fe)-Bearing Sphalerite. *Minerals*, 5 (2): 117–132.

Czamanske, G.K., Kunilov, V.E., Zientek, M.L., Cabri, L.J., Likhachev, A.P., Calk, L.C., and Oscarson, R.L., 1992. A proton-microprobe study of magmatic sulphide ores from the Noril'sk-Talnakh district, Siberia. *The Canadian Mineralogist*, 30: 249–287.

Dare, S.A., Barnes, S.J., Beaudoin, G., Méric, J., Boutroy, E., and Potvin-Doucet, C., 2014. Trace elements in magnetite as petrogenetic indicators. *Mineralium Deposita*, 49(7): 785–796.

Dare, S.A.S., Barnes, S.J., and Beaudoin, G., 2012. Variation in trace element content of magnetite crystallized from a fractionating sulfide liquid, Sudbury, Canada: Implications for provenance discrimination. *Geochimica et Cosmochimica Acta*, 88: 27–50.

Dasch, E.J., 1996. *Encyclopedia of Earth Sciences*. New York: Macmillan Reference USA, 563.

Davy, H., 1983. Contributions on the chemical composition of Precambrian iron formations. In: Trendall, A.F., and Morris, R.C. (ed.), *Iron Formation, Facts and Problems. Development in Precambrian Geology*, Elsevier, 325–344.

De Argollo, R., and Schilling, J.-G., 1978. Ge-Si and Ga-Al fractionation in Hawaiian volcanic rocks. *Geochimica et Cosmochimica Acta*, 42(6): 623–630.

Delvigne, C., Cardinal, D., Hofmann, A., and André, L., 2012. Stratigraphic changes of Ge/Si, REE+ Y and silicon isotopes as insights into the deposition of a Mesoarchaean banded iron formation. *Earth and Planetary Science Letters*, 355: 109–118.

Dupuis, C., and Beaudoin, G., 2011. Discriminant diagrams for iron oxide trace element fingerprinting of mineral deposit types. *Mineralium Deposita*, 46(3): 1–17.

Durif-Varambon, A., Bertaut, E.F., and Pauthenet, R., 1956. Etude des germanates spinelles. *Annali Di Chimica*, 13: 525–543.

Escoube, R., Rouxel, O.J., Edwards, K., Glazer, B., and Donard, O.F., 2015. Coupled Ge/Si and Ge isotope ratios as geochemical tracers of seafloor hydrothermal systems: Case studies at Loihi Seamount and East Pacific Rise 9°50′N. *Geochimica et Cosmochimica Acta*, 167: 93–112.

Faure, G., 1998. *Principles and Applications of Geochemistry* (2nd ed.). New Jersey: Prentice Hall, 928.

Fleet, M.E., 1981. The structure of magnetite. *Acta*

Crystallographica Section B: Structural Crystallography and Crystal Chemistry, 37(4): 917–920.

Frost, B.R., and Lindsley, D.H., 1991. Occurrence of iron-titanium oxides in igneous rocks. *Reviews in Mineralogy and Geochemistry*, 25(1): 433–468.

Gao, J.F., Zhou, M.F., LightFoot, P.C., Wang, C.Y., Qi, L., and Sun, M., 2013. Sulfide saturation and magma emplacement in the formation of the Permian Huangshandong Ni-Cu sulfide deposit, Xinjiang, Northwestern China. *Economic Geology*, 108: 1833–1848.

Höll, R., Kling, M., and Schroll, E., 2007. Metallogenesis of germanium–A review. *Ore Geology Reviews*, 30(3–4): 145–180.

Hörmann, P.K., 1963. Zur geochemie des germaniums. *Geochimica et Cosmochimica Acta*, 27(8): 861–876.

Hamade, T., Konhauser, K.O., Raiswell, R., Goldsmith, S., and Morris, R.C., 2003. Using Ge/Si ratios to decouple iron and silica fluxes in Precambrian banded iron formations. *Geology*, 31(1): 35–38.

Hawley, J.E., and Stanton, R.L., 1962. The Sudbury ores, their mineralogy and origin; Part 2, The facts; The ores, their minerals, metals and distribution. *The Canadian Mineralogist*, 7: 30–145.

Higgins, M.D., 2005. A new interpretation of the structure of the Sept Iles Intrusive suite, Canada. *Lithos*, 83(3–4): 199–213.

Hu Ruizhong, Su Wenchao, Qi Huawen and Bi Xianwu, 2000. Geochemistry, mode of occurrence and metallogenesis of germanium. *Bulletin of Mineralogy, Petrology and Geochemistry*, 19(4): 215–217 (in Chinese).

Huang, X.W., Gao, J.F., Qi, L., Meng, Y.M., Wang, Y.C., and Dai, Z.H., 2016. In-situ LA-ICP-MS trace elements analysis of magnetite: The Fenghuangshan Cu-Fe-Au deposit, Tongling, Eastern China. *Ore Geology Reviews*, 72: 746–759.

Huang, X.W., Gao, J.F., Qi, L., and Zhou, M.F., 2015a. In-situ LA-ICP-MS trace elemental analyses of magnetite and Re–Os dating of pyrite: The Tianhu hydrothermally remobilized sedimentary Fe deposit, NW China. *Ore Geology Reviews*, 65: 900–916.

Huang, X.W., Qi, L., Gao, J.F., and Zhou, M.F., 2013a. First reliable Re-Os ages of pyrite and stable isotope compositions of Fe(-Cu) deposits in the Hami region, Eastern Tianshan Orogenic Belt, NW China. *Resource Geology*, 63(2): 166–187.

Huang, X.W., Zhou, M.F., Qi, L., Gao, J.F., and Wang, Y.W., 2013b. Re-Os isotopic ages of pyrite and chemical composition of magnetite from the Cihai magmatic-hydrothermal Fe deposit, NW China. *Mineralium Deposita*, 48(8): 925–946.

Huang, X.W., Zhou, M.F., Qiu, Y.Z., and Qi, L., 2015b. In-situ LA-ICP-MS trace elemental analyses of magnetite: The Bayan Obo Fe-REE-Nb deposit, North China. *Ore Geology Reviews*, 65: 884–899.

Huang Xiaowen, Qi Liang and Meng Yumiao, 2014a. Trace element geochemistry of magnetite from the Fe(-Cu) deposits in the Hami region, Eastern Tianshan Orogenic Belt, NW China. *Acta Geologica Sinica* (English Edition), 88(1): 176–195.

Huang Xiaowen, Qi Liang, Wang Yichang and Liu Yingying, 2014b. Re-Os dating of magnetite from the Shaquanzi Fe-Cu deposit, eastern Tianshan, NW China. *Science China: Earth Sciences*, 57(2): 267–277.

Kegler, P., and Holzheid, A., 2011. Determination of the formal Ge-oxide species in silicate melts at oxygen fugacities applicable to terrestrial core formation scenarios. *European Journal of Mineralogy*, 23(3): 369–378.

Klein, C., 2005. Some Precambrian banded iron-formations (BIFs) from around the world: Their age, geologic setting, mineralogy, metamorphism, geochemistry, and origins. *American Mineralogist*, 90(10): 1473–1499.

Lindsley, D.H., 1976. The crystal chemistry and structure of oxide minerals as exemplified by the Fe-Ti oxides. In: Rumble III, D. (ed.), *Reviews in Minerals: Oxide Minerals*, Mineralogical Society of America, L1–L60.

Liu, P.P., Zhou, M.F., Chen, W.T., Gao, J.F., and Huang, X.W., 2015. In-situ LA-ICP-MS trace elemental analyses of magnetite: Fe–Ti–(V) oxide-bearing mafic–ultramafic layered intrusions of the Emeishan Large Igneous Province, SW China. *Ore Geology Reviews*, 65: 853–871.

Liu Shaofeng and Fu Shuixing, 2016. A Research Review of Iron Oxide Copper–Gold Deposits. *Acta Geologica Sinica* (English Edition), 90(4): 1341–1352.

Liu, Y., Hu, Z., Gao, S., Günther, D., Xu, J., Gao, C., and Chen, H., 2008. *In situ* analysis of major and trace elements of anhydrous minerals by LA-ICP-MS without applying an internal standard. *Chemical Geology*, 257(1-2): 34–43.

Longerich, H.P., Jackson, S.E., and Günther, D., 1996. Laser ablation inductively coupled plasma mass spectrometric transient signal data acquisition and analyte concentration calculation. *Journal of Analytical Atomic Spectrometry*, 11(9): 899–904.

Malvin, D.J., and Drake, M.J., 1987. Experimental determination of crystal/melt partitioning of Ga and Ge in the system forsterite-anorthite-diopside. *Geochimica et Cosmochimica Acta*, 51(8): 2117–2128.

Mark, G., Oliver, N.H.S., and Williams, P.J., 2006. Mineralogical and chemical evolution of the Ernest Henry Fe oxide–Cu–Au ore system, Cloncurry district, northwest Queensland, Australia. *Mineralium Deposita*, 40(8): 769–801.

McIntire, W.L., 1963. Trace element partition coefficients—a review of theory and applications to geology. *Geochimica et Cosmochimica Acta*, 27(12): 1209–1264.

Mortlock, R.A., and Frohlich, P.N., 1987. Continental weathering of germanium: in the global river discharge. *Geochimica et Cosmochimica Acta*, 51(8): 2075–2082.

Mortlock, R.A., Froelich, P.N., Feely, R.A., Massoth, G.J., Butterfield, D.A., and Lupton, J.E., 1993. Silica and germanium in Pacific Ocean hydrothermal vents and plumes. *Earth and Planetary Science Letters*, 119(3): 365–378.

Nadoll, P., Angerer, T., Mauk, J.L., French, D., and Walshe, J., 2014. The chemistry of hydrothermal magnetite: A review. *Ore Geology Reviews*, 61: 1–32.

Nadoll, P., and Koenig, A.E., 2011. LA-ICP-MS of magnetite: methods and reference materials. *Journal of Analytical Atomic Spectrometry*, 26(9): 1872–1877.

Nadoll, P., Mauk, J.L., Leveille, R.A., and Koenig, A.E., 2015. Geochemistry of magnetite from porphyry Cu and skarn deposits in the southwestern United States. *Mineralium Deposita*, 50(4): 493-515.

Naldrett, A., Singh, J., Krstic, S., and Li, C., 2000. The mineralogy of the Voisey's Bay Ni-Cu-Co deposit, northern Labrador, Canada: Influence of oxidation state on textures and mineral compositions. *Economic Geology*, 95(4): 889–900.

Norman, M.D., Pearson, N.J., Sharma, A., and Griffin, W.L., 1996. Quantitative analysis of trace elements in geological

materials by laser ablation ICPMS: Instrumental operating conditions and calibration values of NIST glasses. *Geostandards and Geoanalytical Research*, 20(2): 247–261.

Ottemann, J., and Nuber, B., 1972. Brunogeierit, ein Germanium-Ferritspinell von Tsumeb. *Neues Jahrbuch fur Mineralogical Monatsch*: 263–267.

Pazenkova, N.I., 1967. Germaniferous limonite-forming mechanism. *Dok. Acad. Sci. USSR, Earth Sci. Sect.*, 173: 204–206 (English translation).

Pokrovski, G.S., and Schott, J., 1998. Thermodynamic properties of aqueous Ge (IV) hydroxide complexes from 25 to 350 C: implications for the behavior of germanium and the Ge/Si ratio in hydrothermal fluids. *Geochimica et Cosmochimica Acta*, 62 (9): 1631–1642.

Pokrovsky, O., Pokrovski, G., Schott, J., and Galy, A., 2006. Experimental study of germanium adsorption on goethite and germanium coprecipitation with iron hydroxide: X-ray absorption fine structure and macroscopic characterization. *Geochimica et Cosmochimica Acta*, 70(13): 3325–3341.

Reimann, C., and Caritat, P.D., 1998. *Chemical elements in the environment*. Berlin, Heidelberg, New York: Springer Verlag.

Righter, K., King, C., Danielson, L., Pando, K., and Lee, C.T., 2011. Experimental determination of the metal/silicate partition coefficient of Germanium: Implications for core and mantle differentiation. *Earth and Planetary Science Letters*, 304(3): 379–388.

Rosenberg, E., 2009. Germanium: environmental occurrence, importance and speciation. *Reviews in Environmental Science and Bio/Technology*, 8(1): 2–57.

Rossiter, M.J., 1966. Mossbauer absorption in some ferrous spinels. *Physics Letters*, 21(2): 128–130.

Rudnick, R.L., and Gao, S., 2003. Composition of the continental crust. In: Holland, H.D., and Turekian, K.K. (ed.), *Treatise on geochemistry*. Oxford: Elsevier-Pergaman, 1–64.

Saprykin, F.Y., 1977. Deposits of germanium. In: Smirnov, V.I. (ed.), *Ore Deposits of the USSR*. New York: Pitman Publishing, 442–451.

Schrön, W., 1968. Ein Beitrag zur Geochemie des Germaniums. I. Petrogenetische Probleme. *Chemie der Erde*, 27: 193–251.

Shannon, R.D., 1976. Revised effective ionic radii and systematic studies of interatomic distances in halides and chalcogenides. *Acta Crystallographica Section A: Crystal Physics, Diffraction, Theoretical and General Crystallography*, 32(5): 751–767.

Taylor, S.R., and McLennan, S.M., 1985. *The continental crust: its composition and evolution*. Palo Alto, CA: Blackwell Scientific Publisher.

Tu Guangchi, 2004. *The geochemistry and ore-forming mechanism of the dispersed elements*. Beijing: Geological Publishing House (in Chinese).

Vakrushev, V.A., and Semenov, V.N., 1969. Regularities of germanium distribution in magnetite of iron-ore deposits (exemplified by the Altai-Sayan region and the Yenisey Ridge). *Geokhimiya*, 6: 683–690 (in Russian with English abstract).

Wang, C.Y., Zhou, M.F., Yang, S., Qi, L., and Sun, Y., 2014. Geochemistry of the Abulangdang intrusion: Cumulates of high-Ti picritic magmas in the Emeishan large igneous province, SW China. *Chemical Geology*, 378: 24–39.

Wang Tianfeng, Zhao Qingle and Wang Qianqian, 2015. Paleozoic Tectono-Metallogeny in the Tianshan-Altay Region, Central Asia. *Acta Geologica Sinica* (English Edition), 89(4): 1120–1132.

Wechsler, B.A., Lindsley, D.H., and Prewitt, C.T., 1984. Crystal structure and cation distribution in titanomagnetites ($Fe_{3-x}Ti_xO_4$). *American Mineralogist*, 69(7–8): 754–770.

Wheat, C.G., and McManus, J., 2008. Germanium in mid‐ocean ridge flank hydrothermal fluids. *Geochemistry, Geophysics, Geosystems*, 9(3): 1–16.

Yi Liwen, Gu Xiangping, Lu Anhuai, Liu Jianping, Lei Hao, Wang Zhiling, Cui Yu, Zuo Hongyan and Shen Can, 2015. Major and Trace Elements of Magnetite from the Qimantag Metallogenic Belt: Insights into Evolution of Ore–forming Fluids. *Acta Geologica Sinica* (English Edition), 89(4): 1226–1243.

Yin Jiangning, Xing Shuwen and Xiao Keyan, 2016. Metallogenic Characteristics and Resource Potential Analysis of the Middle Lower Yangtze River Fe-Cu-Au-Pb-Zn Metallogenic Belt. *Acta Geologica Sinica*, 90(7): 1525–1536 (in Chinese with English Abstract).

Zhao, W.W., and Zhou, M.F., 2015. In-situ LA–ICP-MS trace elemental analyses of magnetite: The Mesozoic Tengtie skarn Fe deposit in the Nanling Range, South China. *Ore Geology Reviews*, 65: 872–883.

Zhao, X.F., Zhou, M.F., Li, J.W., Selby, D., Li, X.H., and Qi, L., 2013. Sulfide Re-Os and Rb-Sr isotope dating of the Kangdian IOCG metallogenic province, southwest China: Implications for regional metallogenesis. *Economic Geology*, 108(6): 1489–1498.

Zhao, X.F., and Zhou, M.F., 2011. Fe-Cu deposits in the Kangdian region, SW China: a Proterozoic IOCG (iron-oxide-copper-gold) metallogenic province. *Mineralium Deposita*, 46 (3): 1–17.

Zhou, M.F., Michael Lesher, C., Yang, Z., Li, J., and Sun, M., 2004. Geochemistry and petrogenesis of 270 Ma Ni-Cu-(PGE) sulfide-bearing mafic intrusions in the Huangshan district, Eastern Xinjiang, Northwest China: implications for the tectonic evolution of the Central Asian orogenic belt. *Chemical Geology*, 209(3–4): 233–257.

Zhou, M.F., Wei, T.C., Wang, C.Y., Prevec, S.A., Liu, P.P., and Howarth, G.H., 2013. Two stages of immiscible liquid separation in the formation of Panzhihua-type Fe-Ti-V oxide deposits, SW China. *Geoscience Frontiers*, 4(5): 481–502.

About the first author

MENG Yumiao was born in Shenyang of China in 1987, and received her Ph.D. from the University of Chinese Academy of Sciences in 2014. She is currently an assistant professor at the State Key Laboratory of Ore Deposit Geochemistry, Institute of Geochemistry, Chinese Academy of Sciences, Guiyang, China. Her research interests focus on the non-traditional stable isotopes (Ge and Sb), in-situ trace elements of sulfides, and ore genesis of the low-temperature Pb-Zn and Au deposits. Email: mengyumiao@vip.gyig.ac.cn.